DOI: 10.1002/asia.200600162

Carbon-Nanotube-Based Hybrid Materials: Nanopeapods

Ryo Kitaura and Hisanori Shinohara*[a]

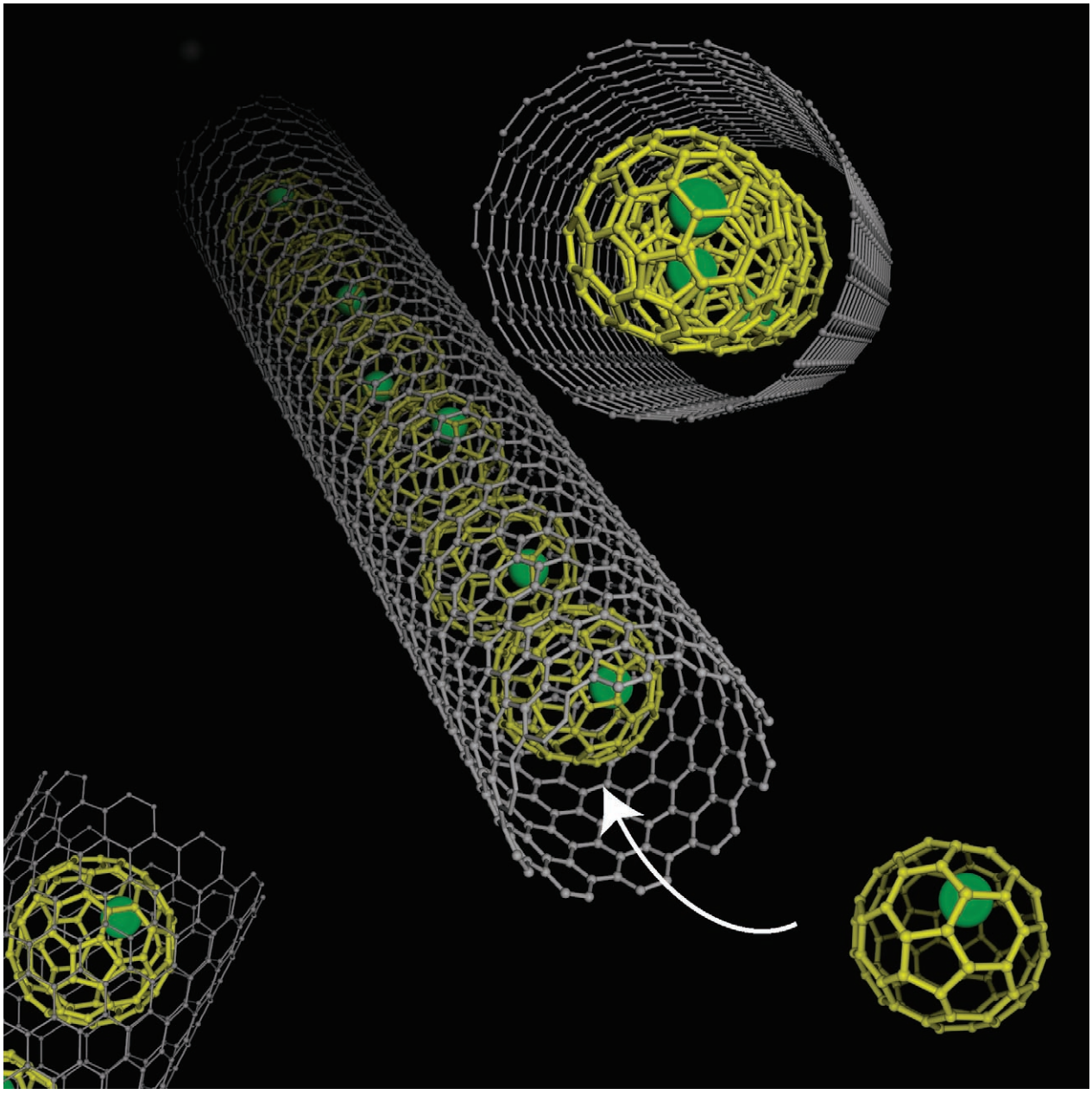

Abstract: This review article focuses on the structures and properties of novel hybrid nanocarbon materials, which are created by incorporating atoms and molecules into the hollow spaces of carbon nanotubes (CNTs); thus they are called nanopeapods. After dealing with synthesis procedures, we discuss the structures and electronic properties of the hybrid materials based on high-resolution transmission electron microscopy (HRTEM), electron energy-loss spectroscopy (EELS), X-ray and electron diffraction, scanning tunneling microscopy (STM), and field-effect transistor transport measurements. Utilization of the low-dimensional nanosized spaces of CNTs to produce novel low-dimensional nanocluster, nanowire, and nanotube materials is also discussed.

Keywords: electron transport · fullerenes · nanopeapods · nanostructures · nanotubes

1. Introduction

Since the discovery of carbon nanotubes (CNTs),[1] their unique structure and properties have prompted tremendous experimental and theoretical studies focused on CNTs and related materials. In the past decade, many extraordinary physical and chemical properties of CNTs, including mechanical,[2,3] photophysical,[4–6] transport,[7–12] and magnetic properties,[13–16] have been elucidated. Among these interesting features, one of the most fascinating is the ability to encapsulate atoms or molecules in their central hollow space, thus providing a brand new class of CNT-based hybrid materials with novel structures and properties.

The filling of the interior space of CNTs was first achieved by Ajayan and Iijima by using multi-walled carbon nanotubes (MWNTs) and Pb metal.[17] They found that air annealing of MWNTs with Pb particles deposited on their surface results in an opening of the ends of the MWNTs and the entrapment of Pb metal atoms inside; the ends of CNTs are usually closed by fullerene hemisphere caps. This phenomenon can be understood as a nanometer-scale capillary condensation, which is essentially equivalent to macroscale capillary condensation (it was later revealed that only materials of relatively low surface tension ($<200\,mN\,m^{-1}$) could be drawn inside MWNTs[18]). The presence of Pb atoms inside nanotubes was clearly evidenced by high-resolution transmission electron microscopy (HRTEM) and energy dispersive X-ray analysis.

The incorporation of fullerene molecules into the hollow space of CNTs was accidentally discovered in 1998.[19] Luzzi and co-workers found that C_{60} molecules were incorporated inside single-walled carbon nanotubes (SWNTs) to form 1D regulated C_{60} arrays, like many peas in a pod, while they were studying purified open-ended SWNTs by TEM. C_{60} molecules, which are usually formed as a by-product during the synthesis of SWNTs, are accidentally encapsulated inside SWNTs during the purification process. This hybrid nanocarbon material has been called "nanopeapod", "nanotube peapod", "fullerene peapod", or merely "peapod". Herein, we refer to them as "nanopeapods". Since the work of Luzzi and co-workers, nanopeapods have attracted the attention of many researchers, owing not only to their unique structures but also to their interesting chemical and physical properties. The development of methods for the synthesis and investigation of nanopeapods under various physical and chemical conditions have made peapod studies one of the most fascinating and advanced areas of CNT research.

2. Synthesis and Structure of Nanopeapods

2.1. Synthesis of Nanopeapods

In the first report by Luzzi and co-workers, the degree of nanotube filling with C_{60} molecules was only about 5%. Since then, a technique has been developed to achieve filling ratios of about 80–85% for C_{60} nanopeapods. The synthesis method is straightforward. Purified fullerenes and open-ended SWNTs are normally vacuum-sealed in a quartz tube, which is heated at 400–600 °C in a vacuum (10^{-5} torr) for two days. At this temperature and pressure, fullerene molecules sublime and enter the hollow spaces of SWNTs

[a] Prof. R. Kitaura, Prof. H. Shinohara
Department of Chemistry and Institute for Advanced Research
Nagoya University
Nagoya 464-8602 (Japan)
Fax: (+81) 52-789-1169
E-mail: noris@cc.nagoya-u.ac.jp

through the open ends. One of the important points in obtaining high-yield filling is that we have to prepare highly pure open-ended SWNTs whose diameters are large enough to encapsulate fullerene molecules. Fullerene molecules have a diameter of about 1 nm, based on the van der Waals radius of carbon atoms (0.34 nm). SWNTs can then be filled with fullerene molecules by using those with diameters on the order of or larger than about 1.38 nm. Nanotubes with such diameters can be synthesized easily by incorporating the laser-ablation (laser-furnace) or arc-discharge method. After the fullerene-insertion process, fullerene molecules adsorbed on the side walls of the SWNTs are removed by ultrasonic cleaning with organic solvents such as toluene and *o*-xylene.

Besides the gas phase, nanopeapods can also be synthesized through liquid-phase reactions. The method involves immersing open-ended SWNTs in a saturated solution of fullerenes. The filling efficiency is not high enough to be comparable to gas-phase filling (70% at most at present).[20,21] The solution method is, however, especially advantageous in the incorporation of thermally unstable or nonvolatile molecules such as biological molecules (e.g., DNA) and polynuclear metal complexes. A further development of the solution method is, therefore, quite important and crucial for expanding the variety of SWNT-based hybrid materials.

Ryo Kitaura *was born in 1974. He studied chemistry and physical chemistry, and received his PhD in 2003 from Kyoto Univ. He then worked at Toyota's central R&D laboratories, and joined Nagoya Univ. in 2005 as an Assist. Prof. in the Physical Chemistry Laboratory, Department of Chemistry. His current research interests focus on the chemistry and physics in the nanosized spaces of nanocarbon materials.*

Hisanori Shinohara *received his BSc in 1977 from Shinshu Univ. and his PhD in chemical physics from Kyoto Univ. in 1983. He joined the research group of Prof. Nishi as a research associate of the Institute for Molecular Science (IMS) at Okazaki in 1979, where he did pioneering work on laser spectroscopy of supersonic jet-cooled molecular clusters. He became an Assoc. Prof. at Mie Univ. in 1988, where he started working on fullerenes and metallofullerenes. He became a Full Prof. at Nagoya Univ. in 1993. He is well-known for his achievements in the production and characterization of endohedral metallofullerenes and novel CNT materials, including nanopeapods.*

2.2. Structure of Nanopeapods

2.2.1. Nanopeapods That Encapsulate Fullerenes

The structure of nanopeapods has been characterized by HRTEM, electron diffraction (ED), and X-ray diffraction (XRD) analyses. A typical HRTEM image and the corresponding structure model of C_{60} nanopeapods are shown in Figure 1 a and b, respectively. Ring-shaped contrasts are attributed to encapsulated C_{60} molecules. Intermolecular distances of the 1D array of C_{60} inside the SWNTs are very uniform, to the extent that a 1D crystal of C_{60} is considered to be formed in the SWNTs.[22,23] Although HRTEM is a very powerful method of observation that provides us with direct local structure information, it is difficult to evaluate the bulk structure. ED and XRD analyses are complementary to HRTEM in giving information about the bulk structure.

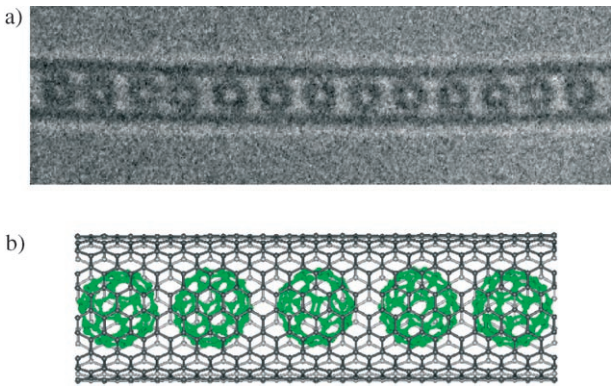

Figure 1. a) Typical HRTEM image of the C_{60} nanopeapods. b) Structure model of the C_{60} nanopeapod based on HRTEM.

According to the regular 1D array of C_{60} molecules in nanopeapods, we can observe new diffraction peak(s) that is/are absent in empty SWNTs.[24,25] Figure 2 shows an electron diffraction pattern of C_{60} nanopeapods; the position of this peak provides information on the intermolecular distances of the encapsulated molecules. Interestingly, the intermolecular distance determined between encapsulated C_{60} molecules is shorter than that of bulk C_{60} crystal; the intermolecular distance of a face-centered cubic (fcc) array of

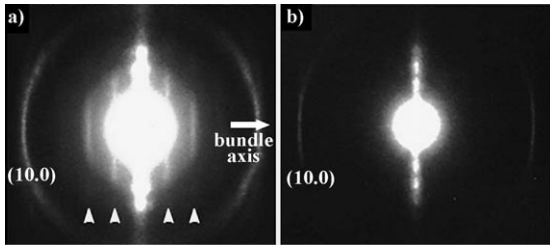

Figure 2. Electron diffraction pattern of a) C_{60} nanopeapods and b) empty SWNT bundle.

bulk C_{60} crystal is 1.00 nm, whereas that of the C_{60} nanopeapod is 0.95 nm.[22] The interaction between the walls of the SWNTs and C_{60} is mainly van der Waals in nature. However, once nanopeapods are formed, their structure becomes very stable due to the formation of a deep interaction potential well resulting from the specific nanostructure of the SWNTs. It is suggested that the deep interaction potential well of SWNTs induces a high-pressure effect towards encapsulated fullerene molecules, which leads to shortening of the intermolecular distances. Theoretical studies predict that the encapsulation process of C_{60} is exothermic for SWNTs of a certain diameter. For example, each C_{60} molecule is stabilized by 0.51 eV upon encapsulation in a (10, 10) SWNT.[26]

2.2.2. Nanopeapods That Encapsulate Endohedral Metallofullerenes

Like C_{60}, metallofullerenes such as $Sc_2@C_{84}$, $Ti_2C_2@C_{78}$, $La@C_{82}$, $La_2@C_{80}$, $Ce_2@C_{80}$, $Ce@C_{82}$, $Sm@C_{82}$, $Gd@C_{82}$, and $Gd_2@C_{92}$ can also form nanopeapods (endohedral metallofullerenes are usually denoted as $M@C_n$, which means that the metal atom M is encapsulated in the C_n fullerene cage).[27–32] Figure 3 shows an HRTEM image of $Gd@C_{82}$

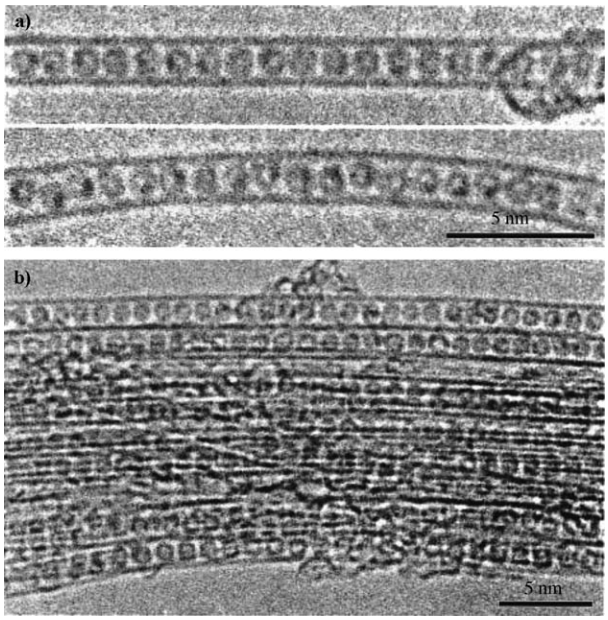

Figure 3. HRTEM image of a) individual and b) bundled $Gd@C_{82}$ nanopeapods.

nanopeapods.[23] The dark spots seen in most of the ring-shaped contrasts are attributed to encapsulated individual Gd metal atoms. It is remarkable that single atoms can be directly observed even at room temperature (Figure 3). The intermolecular distance between encapsulated $Gd@C_{82}$ molecules is 1.1 nm, which is slightly shorter than that of the bulk crystal.

One of the most interesting structural aspects of metallofullerene nanopeapods is the dynamic behavior of metallofullerene molecules in SWNTs. As illustrated in Figure 3, the fact that Gd atoms can be seen by HRTEM indicates that the fullerene cages are not rotating on the timescale of HRTEM, even at room temperature. However, dark spots in some of the ring-shaped contrasts imply that some of the fullerene cages are indeed rotating. An HRTEM analysis of $(Ce@C_{82})_n@SWNT$ revealed that incorporated $Ce@C_{82}$ molecules show translational motion even inside apparently completely filled nanotubes.[33] The 1D $Ce@C_{82}$ crystal chains formed inside the SWNTs undergo cooperative translational motion such that the entire chain shifts in a short period of time without changing the intermolecular separations. This specific motion indicates that the energy barrier needed for lateral motion in SWNTs is relatively small.

In contrast to lateral motion, the rotational motion of $Ce@C_{82}$ is somewhat restricted in SWNTs. A series of successive HRTEM images (with 2-s camera exposure time and $\approx$10-s interval between exposures) revealed that $Ce@C_{82}$ molecules rotate discontinuously in SWNTs; a particular $Ce@C_{82}$ molecule remains stationary at a certain position for several seconds before jumping abruptly to a new stable orientation. In the $Ce@C_{82}$ bulk crystal, $Ce@C_{82}$ molecules freely rotate at temperatures above 80 K.[34] Therefore, this observation shows that the energy barrier for the rotation of $Ce@C_{82}$ molecules in SWNTs is significantly higher than that in the crystal of $Ce@C_{82}$. As opposed to $Ce@C_{82}$ molecules in SWNTs, the electrostatic field in the close-packed crystalline $Ce@C_{82}$ is highly symmetric, resulting in a small energy barrier for rotation. The nearly free rotation of $Ce@C_{82}$ molecules in the crystal of $Ce@C_{82}$ is substantially inhibited in the case of $(Ce@C_{82})_n@SWNT$ as a result of the lowering of the symmetry of the electrostatic potential for each fullerene molecule.

HRTEM observations of rotational motion of encapsulated fullerene molecules were also reported for $Sm@C_{82}$, $La_2@C_{80}$, $Sc_2@C_{84}$, and $Gd_2@C_{92}$, and different rotational behavior was observed for different metallofullerene nanopeapods.[23,30,35–39] These results indicate that one may control the rotational motion of fullerene peas in SWNTs by changing the fullerene molecules, which is important for applications of nanopeapods, such as recording devices and quantum computations.[21]

2.2.3. Nanopeapods That Encapsulate Exohedral Metallofullerenes

In an attempt to synthesize novel nanopeapods, not only endohedral but also exohedral metallofullerenes have been incorporated in SWNTs. $(KC_{60})_n@SWNT$ was synthesized by introducing potassium vapor into the C_{60} nanopeapods. Figure 4 a–c show an HRTEM image, a simulated HRTEM image, and a structure model of $(KC_{60})_n@SWNT$, respectively. Dark spots observed between C_{60} molecules in the SWNTs are due to individual potassium atoms. Doping of potassium atoms into $C_{60}@SWNT$ occurred inhomogeneously, and the potassium atoms seem to be located randomly in the SWNTs. According to this structural feature, the $K–C_{60}$ distances range from 0.6 to 0.8 nm.

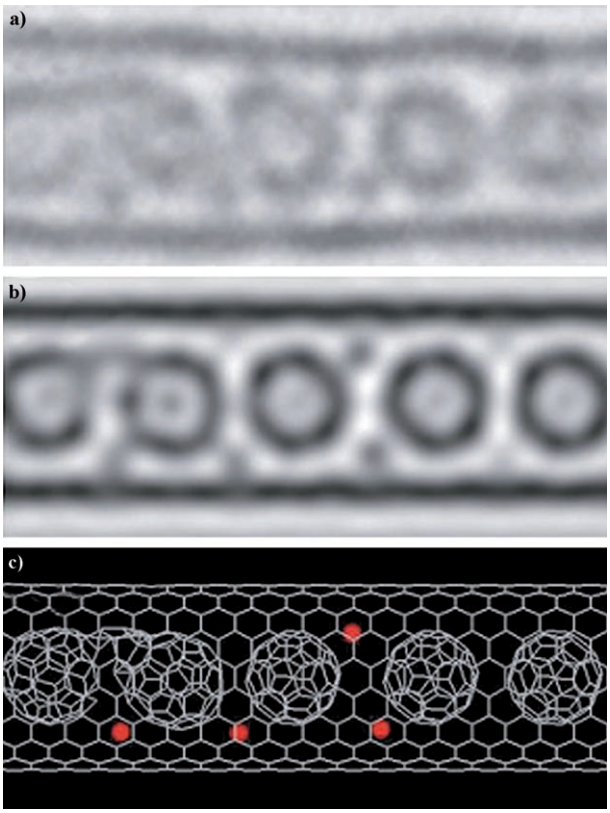

Figure 4. a) Typical HRTEM image of the K-doped C_{60} nanopeapods, b) best-fit simulation based on the structure model in c), and c) its schematic model.

Notably, there is a structural similarity between $(KC_{60})_n$@SWNT peapods and superconducting bulk fullerite crystal, K_3C_{60}. Potassium atoms doped in C_{60} crystals are found in two types of sites: tetrahedral and octahedral. By comparison with K_3C_{60}, the potassium atoms in the peapod occupy sites that are intermediate between tetrahedral and octahedral in nature.

Recently, $(CsC_{60})_n$@SWNT was synthesized by a new chemical-reduction method[40]. In this method, CsC_{60} exohedral metallofullerenes were synthesized first by a reaction between C_{60} and CsOH in THF, then CsC_{60} was doped into SWNTs in a gas-phase reaction. The advantage of this method over the method employed for $(KC_{60})_n$@SWNT synthesis is the following. In the method of alkali-metal sublimation, alkali metals were inserted randomly into the SWNTs and have two different types of positions, intra- and intertubular, where the control of the doping level is very difficult. In contrast, one can control not only the doping level but also the doping positions by using the chemical-reduction method. Figure 5 shows HRTEM images of $(CsC_{60})_n$@SWNT; the Cs atoms are indicated by arrows. The Cs atoms on $(CsC_{60})_n$@SWNT show a stoichiometry of one Cs atom per C_{60} molecule. The Cs atoms and C_{60} molecules can be replaced by other metal atoms and higher fullerenes or even endohedral metallofullerenes, respectively.

In general, exohedral metallofullerenes such as CsC_{60} and KC_{60} are very sensitive to oxidants and are not stable in air

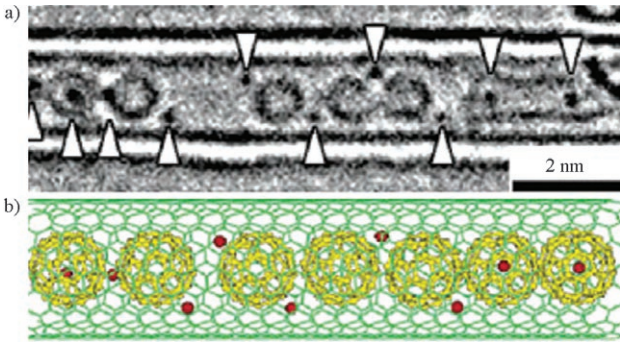

Figure 5. a) HRTEM image of $(CsC_{60})_n$@SWNT nanopeapods with arrows indicating the Cs atoms. b) Schematic representation of the HRTEM image.

and in solvents that contain dioxygen molecules. In contrast, CsC_{60} and K_3C_{60} species in SWNTs are very stable even in air, as these reactive fullerenes are protected from air by the walls of the SWNTs.

3. Properties of Nanopeapods

3.1. Electronic Structures of Nanopeapods

Total-energy electronic-structure calculations of C_{60} nanopeapods with the local density approximation (LDA) in density functional theory were performed by several groups.[26,41,42] The results show that the electronic structure of the peapod is not a simple sum of those of fullerenes and nanotubes. Figure 6 shows the energy-band structure of C_{60} encapsulated in a (10,10) nanotube and that of an isolated (10,10) nanotube. Nearly free electron (NFE) states located between the tube and the fullerenes are found to work as acceptor states that control the relative locations of elec-

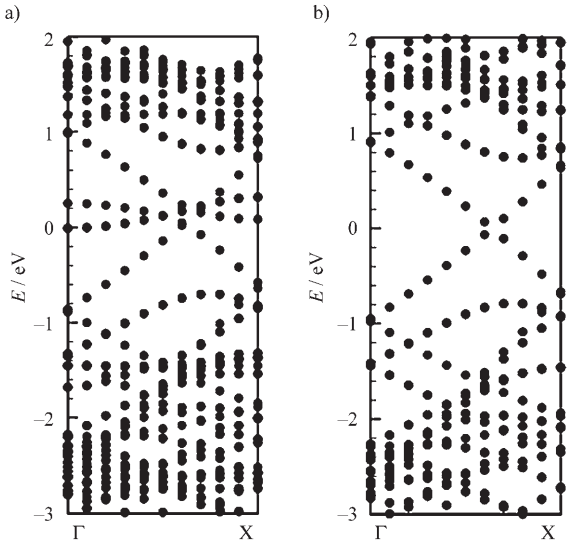

Figure 6. Energy-band structure of a) C_{60} nanopeapods ((10,10) nanotube) and b) isolated nanotube. Energies are measured from the Fermi level.

CHEMISTRY
AN ASIAN JOURNAL

tronic levels and the Fermi energy. As a result, the nanopeapod is a metal with multicarriers, each of which is distributed either on the nanotube or on the 1D chain of the C_{60} fullerenes.

The rotation of the incorporated C_{60} fullerenes can affect the electronic properties of the peapod because the orbital hybridization between fullerene molecules and SWNTs depends on the orientation of the former inside the latter; so do overlapping integrals. By using the Slater–Koster tight-binding calculation, it was found that rotation of the encapsulated C_{60} in the space of a (10,10) tube induces a small energy change,[43] and that the calculated density of states varies depending on the orientational order of the C_{60} molecules. Therefore, we can expect that the novel electronic properties of nanopeapods correlate with the rotation of the fullerene pea. For example, a change in the electronic properties triggered by an external field is expected. In the case of metallofullerenes, an electric or magnetic field can induce an orientational change in the incorporated metallofullerenes owing to their dipole moments and magnetic anisotropy, which results in a change in electronic properties such as electrical conductivity.

The electronic properties of the metal atom of a metallofullerene encapsulated in an SWNT were investigated by electron energy-loss spectroscopy (EELS).[35,44] The peak positions of the *M* edge of the rare-earth-metal atoms are a good indicator of the valence (oxidation) state, and, consequently, one can obtain information on the amount of charge transfer from metal atoms to fullerene cages and SWNT walls.

Figure 7 shows EELS spectra of a bundle of $(Gd@C_{82})_n$@SWNT and of Gd^{3+} in $Gd@C_{82}$. The peak positions of the M_4 and M_5 edges of the Gd atom in $Gd@C_{82}$ are 1184 and 1214 eV, respectively. This peak position is very similar to that of $(Gd@C_{82})_n$@SWNT, which indicates that the valence state of the Gd atom of $(Gd@C_{82})_n$@SWNT is the same as that of $Gd@C_{82}$, and that encapsulation into SWNTs does not change the valence state of the Gd atoms. Similar investigations were carried out for other nanopeapods, and the valence state of rare-earth metals does not vary upon incorporation into SWNTs: +2 for Sc, Ti, and Sm, +3 for other rare-earth metals.

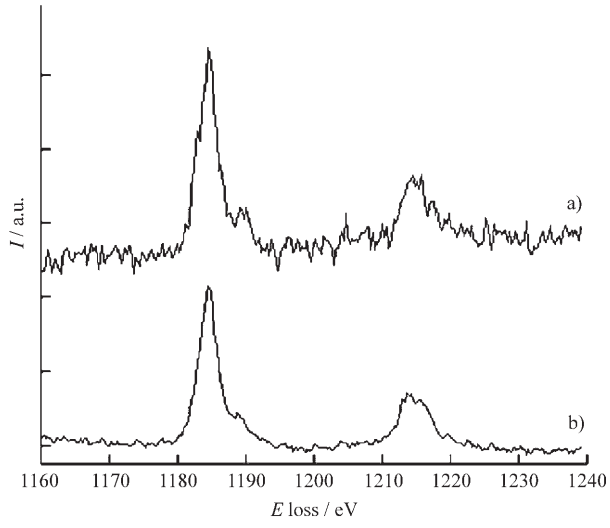

Figure 7. EELS spectrum of a) a bundle of $(Gd@C_{82})$@SWNT and b) Gd^{3+} in $Gd@C_{82}$. In this region, the Gd M_{45} absorption edges are clearly observed.

In contrast to the valence state, the electronic structure of SWNTs is significantly affected by incorporation of fullerene molecules, as revealed by low-temperature scanning tunneling microscopy (STM) and scanning tunneling spectroscopy (STS).[45] Figure 8 shows a typical STM image and the corresponding STS measurements of $(Gd@C_{82})_n$@SWNT; STS shows the spatial variation of d*I*/d*V* along the tube axis, which corresponds to the local density of the states (LDS) of $(Gd@C_{82})_n$@SWNT near the Fermi level. Two strong van Hove singularity (VHS) peaks corresponding to conduction and valence-band edges are clearly seen, and the local band gap is easily evaluated by the width of these two VHS peaks. As clearly illustrated in Figure 8, the band gap is significantly modulated along the tube axis, and the original band gap of the SWNT (0.43 eV) is narrowed to 0.17 eV where the fullerene is expected to be located.

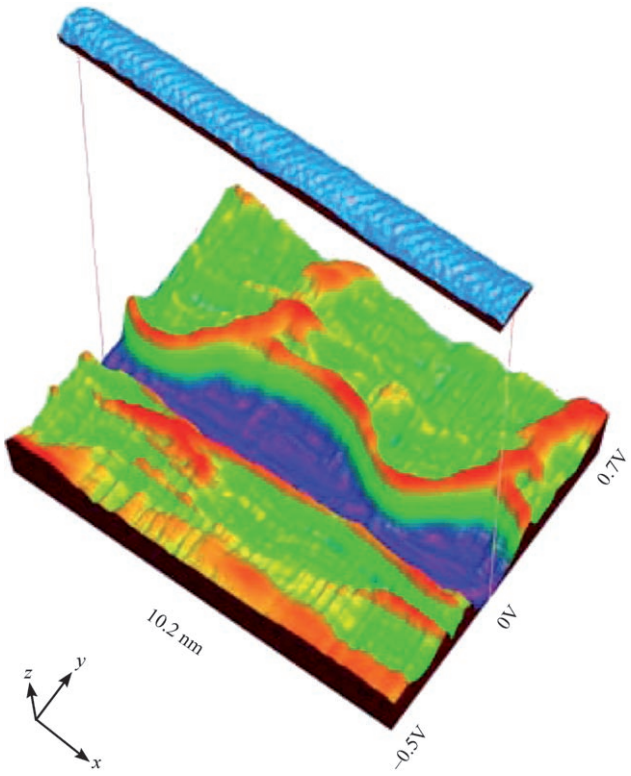

Figure 8. 3D STS representation of an (11,9) SWNT (with $Gd@C_{82}$) topograph, 10.2 nm long in cyan. The corresponding 512 d*I*/d*V* spectrum of the center of the tube is shown for all positions along the tube. The *x* axis indicates the position along the tube, the *y* axis the energy, and the *z* axis d*I*/d*V*. The value of d*I*/d*V* (local density of states) decreases in going from red to green to blue.

This band-gap modulation is explained by the interaction and orbital hybridization between the NFE state of the SWNTs (which has maximum electron density inside the hollow space of SWNTs) and the p orbitals of the fullerene molecules. The degree of interaction depends on the type of encapsulated fullerene molecule and the chirality of the SWNT. Therefore, we can perform "local band-gap engineering" at the site where a fullerene molecule is inserted, which leads to applications as novel electric devices.

3.2 Transport Properties of Nanopeapods

The band-gap modulation discussed above causes a remarkable change in the transport properties of SWNTs. The electronic transport properties of hollow SWNTs and several nanopeapods, $(C_{60})_n$@SWNT, $(C_{78})_n$@SWNT, $(C_{90})_n$@SWNT, $(Gd@C_{82})_n$@SWNT, and $(Dy@C_{82})_n$@SWNT, were investigated by using these compounds as channels of field-effect transistors (FETs); we can evaluate the transport properties of a single bundle of SWNT and nanopeapod by using SWNT and nanopeapod FETs.[29,44,46]

The measured drain current versus gate voltage (I_D vs. V_{GS}, $-40 < V_{GS} < 40$ V) curve for a hollow SWNT FET (diameter of SWNT ≈ 1.4 nm) indicates that SWNT FETs are *p*-type dominated by hole transport, whereas nanopeapod FETs show completely different transport behavior. Figure 9

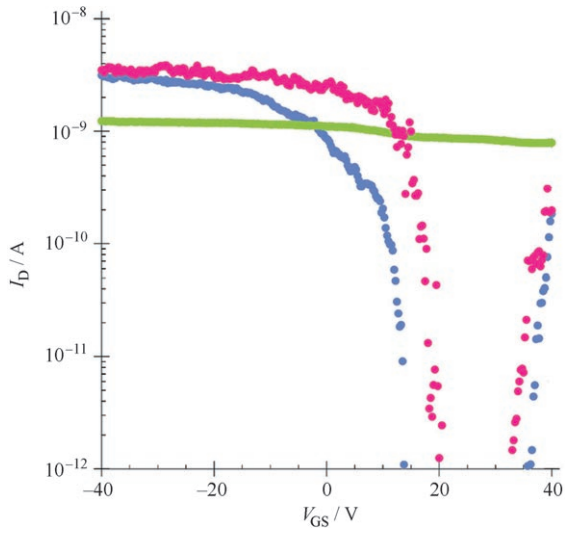

Figure 9. The I_D versus V_{GS} FET curves for C_{90}@SWNT (green), C_{78}@SWNT (blue), and $(Dy@C_{82})$@SWNT (red) at $V_{DS} = 20$ mV, $T = 23$ K. V_{DS} = source-drain voltage.

shows the I_D versus V_{GS} curves for $(C_{90})_n$@SWNT, $(C_{78})_n$@SWNT, and $(Dy@C_{82})_n$@SWNT. As illustrated, $(C_{90})_n$@SWNT exhibited metallic behavior without any pinch-off (insulating) region. However, in the case of $(C_{78})_n$@SWNT, the curve shows a distinct off state, hole transport, and electron transport for $10 < V_{GS} < 30$ V, $V_{GS} < 10$ V, and $V_{GS} > 30$ V, respectively. This result implies that $(C_{78})_n$@SWNT exhibits ambipolar FET behavior with both *n* and *p* channels easily accessible by simple electrostatic gates. Similar ambipolar behavior was observed for $(Dy@C_{82})_n$@SWNT, apart from the width of the off-state voltage (22 and 14 V for $(C_{78})_n$@SWNT and $(Dy@C_{82})_n$@SWNT, respectively). Table 1 summarizes the width of the insulating regions and the diameters for all the nanopeapods investigated.

Table 1. The average width of the insulating regions and the diameters of the fullerene peas for all the nanopeapods.

Pea	C_{60}	C_{78}	C_{90}	$Gd@C_{82}$	$Dy@C_{82}$
ΔV_{GS} [V]	25	22	0	15	14
d [nm]	0.71	0.81	0.87	0.83	0.83

The observed difference in the FET characteristics discussed above can be understood as follows. A semiconducting SWNT with a diameter of about 1.4 nm has a band gap of around 0.6 eV. Therefore, to act as an *n*-type channel, sufficiently high gate voltages are needed to shift down the conduction band of the SWNT electrostatically. As a result, SWNT FETs normally show only *p*-type behavior under the measuring conditions ($-40 < V_{GS} < 40$ V). In contrast, the band gaps of SWNTs are significantly perturbed by the enclosed fullerene peas, thus resulting in smaller band gaps than that of hollow SWNTs; as discussed in the previous section, STS studies clearly revealed local band-gap modulation of nanopeapods.

In the case of $(Gd@C_{82})_n$@SWNT, the band gap is narrowed to 0.17 eV at the sites where $Gd@C_{82}$ molecules are incorporated. This small band gap can lead to carrier transport through both the conduction and valence bands, which results in ambipolar FET behavior. As the degree of band-gap modulation of metallofullerene peapods is much larger than that of hollow fullerene peapods, the former contain a smaller band-gap (smaller insulating) region, as illustrated in Table 1.

Control of transport properties by encapsulation can be obtained not only by fullerenes but also by various organic compounds.[47] Electron-acceptor or -donor molecules such as tetrakis(dimethylamino)ethylene (TDAE), tetramethyltetraselenafulalene (TMTSF), tetracene, anthracene, tetracyano-*p*-quinodimethane (TCNQ), and tetrafluorotetracyano-*p*-quinodimethane (F_4TCNQ) have been utilized as doping agents. These molecules are incorporated into SWNTs by a gas-phase reaction. The charge transfer between SWNTs and incorporated organic molecules is controlled by the ionization energy (IE) or the electron affinity (EA) of the guests; the charge transfer occurs discontinuously at a critical value of IE or EA. Although the EA of C_{60} and TCNQ are very close to each other (2.65 and 2.80 eV, respectively), charge transfer occurs only in $(TCNQ)_n$@SWNT. Resistivity measurements on $(TCNQ)_n$@SWNT films by the four-probe method revealed that the resistance of $(TCNQ)_n$@SWNT is smaller than that of the hollow SWNT by approximately a factor of two at

CHEMISTRY
AN ASIAN JOURNAL

room temperature. A similar decrease in resistance was observed for $(TDAE)_n$@SWNT, $(TTF)_n$@SWNT (TTF = tetrathiafulvalene), $(TMTSF)_n$@SWNT, and $(F_4TCNQ)_n$@SWNT, which is indicative of charge transfer resulting in doping electrons or holes to SWNTs. $(TTF)_n$@SWNT and $(TMTSF)_n$@SWNT FETs showed *n*-type action, whereas $(TCNQ)_n$@SWNT FET showed *p*-type action.

4. Formation of Nanocluster, Nanowire, and Nanotube Materials in CNTs

CNTs can be used as templates not only for 1D arrays of fullerene molecules, but also for various nanocluster, nanowire, and nanotube materials. Due to the restricted 1D space of CNTs, their internal van der Waals surface may regulate the growth behavior of encapsulated materials in a very precise fashion. In this sense, low-dimensional materials synthesized in CNTs are usually hard to prepare by conventional bulk syntheses, and novel materials with specific low-dimensional structures and properties can be created by using the nanospaces of CNTs.

A fusion reaction of fullerene peas in SWNTs can be utilized to synthesize novel carbon cluster materials. Figure 10

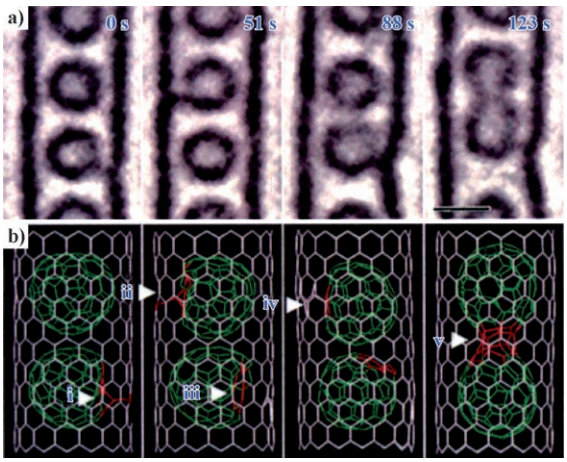

Figure 10. a) Time-dependent HRTEM images of the C_{92}-containing SWNT. b) The corresponding structure models.

shows a series of sequential HRTEM images of $(C_{92})_n$@SWNT with corresponding schematic representations.[48] At the beginning of the observation ($t = 0$ and 51 s), the interlayer coupling between the wall of the SWNT and the C_{92} molecules, which is caused by the induced atomic defect on the fullerene cage, was detected. At $t = 88$ s, two of the interlayer couplings dissociated, and the defects appeared to mend; then the two defect fullerene molecules started to coalesce and form a stable peanutlike large fullerene ($t = 123$ s). The presence of the pentagons of the fullerene cage is one of the important reasons why the atomic defect is more likely to be induced at the fullerene site, although the SWNT wall is more resistive.

Figure 11 shows HRTEM images of an individual Gd mono- and dimetallofullerene encapsulating SWNT

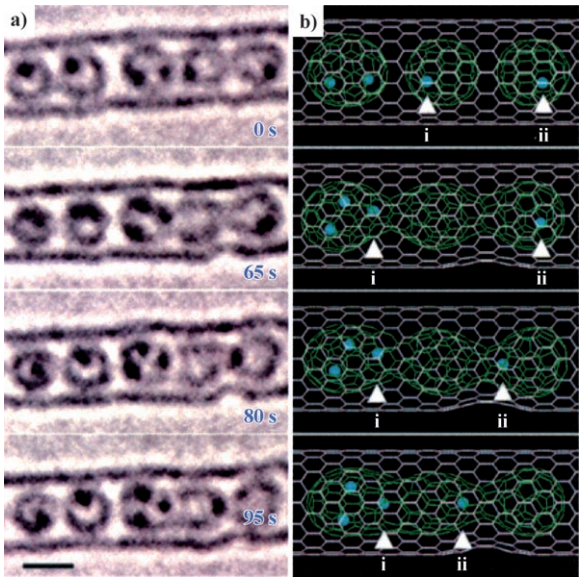

Figure 11. a) A series of HRTEM images of the $Gd@C_{82}$- and $Gd_2@C_{92}$-encapsulating SWNT. b) The corresponding structure models.

$(((Gd_2@C_{92})_{n1},(Gd@C_{82})_{n2})_n$@SWNT) at the beginning of the observation. At first, Gd metallofullerenes are aligned in a 1D way with an almost constant intermolecular spacing. After irradiation for 65 s, the molecules began to coalesce in the SWNT. Then one Gd atom moved into the left cage through the induced atomic path connecting the two cages. Further exposure resulted in coalescence or fusion, which generated a fused peanutlike trimer encapsulating four Gd atoms inside. Similar experiments were also carried out on $(Sm@C_{82})_n$@SWNT.[36] Not only did the fusion reaction take place, a polymerization reaction of the fullerene molecules also occured in the low-dimensional spaces of the SWNTs.[49] When potassium atoms are doped into $(C_{60})_n$@SWNT, an electron transfer from the doped potassium atom to the encapsulated C_{60} molecules initiated polymerization of C_{60} to form 1D C_{60} polymer chains in the SWNTs. Resistivity measurements showed that the C_{60} polymer chain formed in SWNTs has metallic character. The electronic configuration of C_{60} in the polymer chain was presumed to be C_{60}^{6-} from Raman spectra and theoretical calculations.[49]

A novel, low-dimensional ice phase was predicted inside SWNTs by molecular dynamics simulations and confirmed by synchrotron XRD measurements.[24,50,51] XRD studies revealed that confined water molecules inside SWNTs (average diameter 1.37 nm) behave as in the liquid state at room temperature. As the temperature decreases, the confined liquidlike water molecules transform into a crystalline ordered phase, the so-called ice nanotube, at 235 K. Figure 12

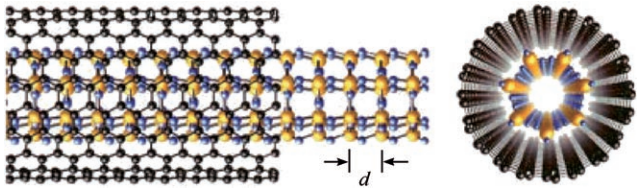

Figure 12. Structure model of ice nanotubes formed in SWNTs.

shows the structure of an ice nanotube, which was proposed based on the simulation of observed XRD patterns. The heptagonal ice nanotubes satisfy the "bulk-ice rule": each oxygen atom has two donors and two acceptors of hydrogen in a known four-coordinate configuration. The formation of heptagonal ice nanotubes was observed at ambient pressure. Although the computer simulations seem to coincide well with the experimental results, the simulations were performed under axial pressures of 50–500 MPa. Structural transition temperatures range from 190 K for octagonal to 300 K for pentagonal ice nanotubes when the diameter of the SWNT is decreased.

Sloan and co-workers prepared various metal-halide nanostructures in CNTs and characterized the structures by HRTEM.[52,53] For example, "all-surface" 2×2 KI crystals within 1.4-nm diameter SWNTs were reported. HRTEM images showed that all the ions undergo a total decrease in coordination from 6:6 to 4:4 resulting from the restricted space of the SWNTs. Lattice distortions were also observed in these 2×2 crystals. ED measurements along the SWNT showed that the spots are spaced at average intervals of about 0.35 nm, which corresponds to the {200} spacing of cubic bulk KI crystals, whereas across the SWNT the spacing increased to about 0.4 nm, which represents a roughly 14% tetragonal distortion.

Another interesting 1D metal-halide chain is cobalt iodide in the SWNTs.[54] The encapsulated cobalt iodide has a 1D complex helix rotated structure, which is unique and unrelated to the bulk state. The diameter of the SWNT varies from 1.1 to 1.3 nm according to the rotational orientation of encapsulated cobalt iodide nanostructures. The restricted space in the SWNT and the strong interaction between the encapsulated material and the encapsulating SWNT play an important role in the formation of such unusual structures.

5. Summary

Various nanopeapods have been synthesized and structurally characterized, and their structure and properties have been discussed. These hybrid materials have properties that are not a simple sum of the encapsulated species and the encapsulating fullerenes or CNTs. Finally, recent progress in the synthesis of novel low-dimensional materials inside CNTs was mentioned. As a result of their well-defined and comparatively simple atomic structure, CNTs can be regarded as excellent templates not only for the creation of novel low-dimensional materials with useful properties, but also for the exploration of theoretical concepts in the physics, chemistry, and materials science of low-dimensional systems. The inner hollow space of CNTs will continue to provide an excellent field for further research in nanometer-scale science and technology.

Acknowledgements

We thank Prof. S. Iijima, Prof. S. Bandow, Dr. K. Hirahara, Dr. T. Okazaki, Dr. K. Suenaga (AIST), Dr. Y. Ohno, Prof. T. Mizutani, Dr. T. Shimada, Dr. T. Sugai (Nagoya University), and Prof. Y. Kuk (Seoul National University) for their useful discussions and collaboration. This work was supported by the JST CREST Program for Novel Carbon Nanotube Materials.

[1] S. Iijima, *Nature* **1991**, *354*, 56–58.
[2] R. H. Baughman, C. Cui, A. A. Zakhidov, Z. Iqbal, J. N. Barisci, G. M. Spinks, G. G. Wallace, A. Mazzoldi, D. De Rossi, A. G. Rinzler, O. Jaschinski, S. Roth, M. Kertesz, *Science* **1999**, *284*, 1340–1344.
[3] J. Bernholc, C. Brabec, M. B. Nardelli, A. Maiti, C. Roland, B. I. Yakobson, *Appl. Phys. A* **1998**, *67*, 39–46.
[4] A. M. Rao, E. Richter, S. Bandow, B. Chase, P. C. Eklund, K. A. Williams, S. Fang, K. R. Subbaswamy, M. Menon, A. Thess, R. E. Smalley, G. Dresselhaus, M. S. Dresselhaus, *Science* **1997**, *275*, 187–191.
[5] R. Saito, M. Fujita, G. Dresselhaus, M. S. Dresselhaus, *Appl. Phys. Lett.* **1992**, *60*, 2204–2206.
[6] M. J. O'Connell, S. M. Bachilo, C. B. Huffman, V. C. Moore, M. S. Strano, E. H. Haroz, K. L. Rialon, P. J. Boul, W. H. Noon, C. Kittrell, J. P. Ma, R. H. Hauge, R. B. Weisman, R. E. Smalley, *Science* **2002**, *297*, 593–596.
[7] A. Javey, J. Guo, Q. Wang, M. Lundstrom, H. J. Dai, *Nature* **2003**, *424*, 654–657.
[8] K. Shibata, Y. Kubozono, T. Kanbara, T. Hosokawa, A. Fujiwara, Y. Ito, H. Shinohara, *Appl. Phys. Lett.* **2004**, *84*, 2572–2574.
[9] S. Margadonna, K. Prassides, *J. Solid State Chem.* **2002**, *168*, 639–652.
[10] J. González, *Phys. Rev. B* **2003**, *67*, 014528.
[11] R. S. Lee, H. J. Kim, J. E. Fischer, A. Thess, R. E. Smalley, *Nature* **1997**, *388*, 255–257.
[12] M. Bockrath, D. H. Cobden, P. L. McEuen, N. G. Chopra, A. Zettl, A. Thess, R. E. Smalley, *Science* **1997**, *275*, 1922–1925.
[13] A. P. Ramirez, R. C. Haddon, O. Zhou, R. M. Fleming, J. Zhang, S. M. Mcclure, R. E. Smalley, *Science* **1994**, *265*, 84–86.
[14] S. Zaric, G. N. Ostojic, J. Kono, J. Shaver, V. C. Moore, M. S. Strano, R. H. Hauge, R. E. Smalley, X. Wei, *Science* **2004**, *304*, 1129–1131.
[15] S. Bandow, S. Asaka, X. Zhao, Y. Ando, *Appl. Phys. A* **1998**, *67*, 23–27.
[16] S. Bandow, F. Kokai, K. Takahashi, M. Yudasaka, S. Iijima, *Appl. Phys. A* **2001**, *73*, 281–285.
[17] P. M. Ajayan, S. Iijima, *Nature* **1993**, *361*, 333–334.
[18] E. Dujardin, T. W. Ebbesen, H. Hiura, K. Tanigaki, *Science* **1994**, *265*, 1850–1852.
[19] B. W. Smith, M. Monthioux, D. E. Luzzi, *Nature* **1998**, *396*, 323–324.
[20] M. Yudasaka, K. Ajima, K. Suenaga, T. Ichihashi, A. Hashimoto, S. Iijima, *Chem. Phys. Lett.* **2003**, *380*, 42–46.
[21] F. Simon, H. Kuzmany, H. Rauf, T. Pichler, J. Bernardi, H. Peterlik, L. Korecz, F. Fulop, A. Janossy, *Chem. Phys. Lett.* **2004**, *383*, 362–367.
[22] K. Hirahara, S. Bandow, K. Suenaga, H. Kato, T. Okazaki, H. Shinohara, S. Iijima, *Phys. Rev. B* **2001**, *6411*, 115420.
[23] K. Hirahara, K. Suenaga, S. Bandow, H. Kato, T. Okazaki, H. Shinohara, S. Iijima, *Phys. Rev. Lett.* **2000**, *85*, 5384–5387.

[24] Y. Maniwa, H. Kataura, M. Abe, A. Fujiwara, R. Fujiwara, H. Kira, H. Tou, S. Suzuki, Y. Achiba, E. Nishibori, M. Takata, M. Sakata, H. Suematsu, *J. Phys. Soc. Jpn.* **2003**, *72*, 45–48.
[25] M. Abe, H. Kataura, H. Kira, T. Kodama, S. Suzuki, Y. Achiba, K. Kato, M. Takata, A. Fujiwara, K. Matsuda, Y. Maniwa, *Phys. Rev. B* **2003**, *68*, 041405.
[26] S. Okada, S. Saito, A. Oshiyama, *Phys. Rev. Lett.* **2001**, *86*, 3835–3838.
[27] B. Y. Sun, T. Inoue, T. Shimada, T. Okazaki, T. Sugai, K. Suenaga, H. Shinohara, *J. Phys. Chem. B* **2004**, *108*, 9011–9015.
[28] T. Okazaki, T. Shimada, K. Suenaga, Y. Ohno, T. Mizutani, J. Lee, Y. Kuk, H. Shinohara, *Appl. Phys. A* **2003**, *76*, 475–478.
[29] T. Shimada, Y. Ohno, T. Okazaki, T. Sugai, K. Suenaga, S. Kishimoto, T. Mizutani, T. Inoue, R. Taniguchi, N. Fukui, H. Okubo, H. Shinohara, *Phys. E* **2004**, *21*, 1089–1092.
[30] K. Suenaga, T. Okazaki, C. R. Wang, S. Bandow, H. Shinohara, S. Iijima, *Phys. Rev. Lett.* **2003**, *90*, 055506.
[31] T. Okazaki, K. Suenaga, Y. F. Lian, Z. N. Gu, H. Shinohara, *J. Mol. Graphics Modell.* **2001**, *19*, 244–251.
[32] B. P. Cao, M. Hasegawa, K. Okada, T. Tomiyama, T. Okazaki, K. Suenaga, H. Shinohara, *J. Am. Chem. Soc.* **2001**, *123*, 9679–9680.
[33] A. N. Khlobystov, K. Porfyrakis, M. Kanai, D. A. Britz, A. Ardavan, H. Shinohara, T. J. S. Dennis, G. A. D. Briggs, *Angew. Chem.* **2004**, *116*, 1410–1413; *Angew. Chem. Int. Ed.* **2004**, *43*, 1386–1389.
[34] W. Sato, K. Sueki, K. Kikuchi, K. Kobayashi, S. Suzuki, Y. Achiba, H. Nakahara, Y. Ohkubo, F. Ambe, K. Asai, *Phys. Rev. Lett.* **1998**, *80*, 133–136.
[35] T. Okazaki, K. Suenaga, K. Hirahara, S. Bandow, S. Iijima, H. Shinohara, *Phys. B* **2002**, *323*, 97–99.
[36] T. Okazaki, K. Suenaga, K. Hirahara, S. Bandow, S. Iijima, I. E. Shinohara, *J. Am. Chem. Soc.* **2001**, *123*, 9673–9674.
[37] K. Suenaga, T. Tencé, C. Mory, C. Colliex, H. Kato, T. Okazaki, H. Shinohara, K. Hirahara, S. Bandow, S. Iijima, *Science* **2000**, *290*, 2280–2282.
[38] B. W. Smith, D. E. Luzzi, Y. Achiba, *Chem. Phys. Lett.* **2000**, *331*, 137–142.
[39] K. Suenaga, R. Taniguchi, T. Shimada, T. Okazaki, H. Shinohara, S. Iijima, *Nano Lett.* **2003**, *3*, 1395–1398.
[40] B. Y. Sun, Y. Sato, K. Suenaga, T. Okazaki, N. Kishi, T. Sugai, S. Bandow, S. Iijima, H. Shinohara, *J. Am. Chem. Soc.* **2005**, *127*, 17972–17973.
[41] O. Dubay, G. Kresse, *Phys. Rev. B* **2004**, *70*, 165424.
[42] Y. Cho, S. Han, G. Kim, H. Lee, J. Ihm, *Phys. Rev. Lett.* **2003**, *90*, 106402.
[43] J. Chen, J. Dong, *J. Phys. Condens. Matter* **2004**, *16*, 1401–1408.
[44] T. Okazaki, T. Shimada, K. Suenaga, Y. Ohno, T. Mizutani, J. Lee, Y. Kuk, H. Shinohara, *Appl. Phys. A* **2003**, *76*, 475–478.
[45] J. Lee, H. Klm, S. J. Kahng, G. Klm, Y. W. Son, J. Ihm, H. Kato, Z. W. Wang, T. Okazaki, H. Shinohara, Y. Kuk, *Nature* **2002**, *415*, 1005–1008.
[46] T. Shimada, Y. Ohno, K. Suenaga, T. Okazaki, S. Kishimoto, T. Mizutani, R. Taniguchi, H. Kato, B. P. Cao, T. Sugai, H. Shinohara, *Jpn. J. Appl. Phys. Part 1* **2005**, *44*, 469–472.
[47] T. Takenobu, T. Takano, M. Shiraishi, Y. Murakami, M. Ata, H. Kataura, Y. Achiba, Y. Iwasa, *Nat. Mater.* **2003**, *2*, 683–688.
[48] K. Urita, Y. Sato, K. Suenaga, A. Gloter, A. Hashimoto, M. Ishida, T. Shimada, H. Shinohara, S. Iijima, *Nano Lett.* **2004**, *4*, 2451–2454.
[49] T. Pichler, H. Kuzmany, H. Kataura, Y. Achiba, *Phys. Rev. Lett.* **2001**, *87*, 267401.
[50] Y. Maniwa, H. Kataura, M. Abe, S. Suzuki, Y. Achiba, H. Kira, K. Matsuda, *J. Phys. Soc. Jpn.* **2002**, *71*, 2863–2866.
[51] Y. Maniwa, H. Kataura, M. Abe, A. Udaka, S. Suzuki, Y. Achiba, H. Kira, K. Matsuda, H. Kadowaki, Y. Okabe, *Chem. Phys. Lett.* **2005**, *401*, 534–538.
[52] J. Sloan, A. I. Kirkland, J. L. Hutchison, M. L. H. Green, *Acc. Chem. Res.* **2002**, *35*, 1054–1062.
[53] J. L. Hutchison, J. Sloan, A. I. Kirkland, M. L. H. Green, *J. Electron Microsc.* **2004**, *53*, 101–106.
[54] E. Philp, J. Sloan, A. I. Kirkland, R. R. Meyer, S. Friedrichs, J. L. Hutchison, M. L. H. Green, *Nat. Mater.* **2003**, *2*, 788–791.

Received: May 26, 2006
Published online: October 13, 2006

